J. Fluid Mech. (1988), *vol.* 189, *pp.* 463–489
Printed in Great Britain

The unsteady force on a body at low Reynolds number; the axisymmetric motion of a spheroid

By C. J. LAWRENCE
Department of Theoretical and Applied Mechanics, University of Illinois at Urbana-Champaign, 216 Talbot Laboratory, 104 South Wright Street, Urbana, IL 61801, USA

AND S. WEINBAUM
Department of Mechanical Engineering, The City College of the City University of New York, New York, NY 10031, USA

(Received 14 June 1986 and in revised form 14 September 1987)

In a recent paper by Lawrence & Weinbaum (1986) an unexpected new behaviour was discovered for a nearly spherical body executing harmonic oscillations in unsteady Stokes flow. The force was not a simple quadratic function in half-integer powers of the frequency parameter $\lambda^2 = -ia^2\omega/\nu$, as in the classical solution of Stokes (1851) for a sphere, and the force for an arbitrary velocity $U(t)$ contained a new memory integral whose kernel differed from the classical $t^{-\frac{1}{2}}$ behaviour derived by Basset (1888) for a sphere. A more general analysis of the unsteady Stokes equations is presented herein for the axisymmetric flow past a spheroidal body to elucidate the behaviour of the force at arbitrary aspect ratio. Perturbation solutions in the frequency parameter λ are first obtained for a spheroid in the limit of low- and high-frequency oscillations. These solutions show that in contrast to a sphere the first-order corrections for the component of the drag force that is proportional to the first power of λ exhibit a different behaviour in the extreme cases of the steady Stokes flow and inviscid limits. Exact solutions are presented for the middle frequency range in terms of spheroidal wave functions and these results are interpreted in terms of the analytic solutions for the asymptotic behaviour. It is shown that the force on a body can be represented in terms of four contributions; the classical Stokes and virtual mass forces; a newly defined generalized Basset force proportional to λ whose coefficient is a function of body geometry derived from the perturbation solution for high frequency; and a fourth term which combines frequency and geometry in a more general way. In view of the complexity of this fourth term, a relatively simple correlation is proposed which provides good accuracy for all aspect ratios in the range $0.1 < b/a < 10$ where exact solutions were calculated and for all values of λ. Furthermore, the correlation has a simple inverse Laplace transform, so that the force may be found for an arbitrary velocity $U(t)$ of the spheroid. The new fourth term transforms to a memory integral whose kernel is either bounded or has a weaker singularity than the $t^{-\frac{1}{2}}$ behaviour of the Basset memory integral. These results are used to propose an approximate functional form for the force on an arbitrary body in unsteady motion at low Reynolds number.

1. Introduction

The oscillatory motion of particles at low Reynolds number is of interest in Brownian motion, suspension rheometry and the passage of sound waves through particulate systems. More general unsteady particle motions occur for interactions in

colloidal suspensions, for particles in filters and for particles in turbulent flow. This paper will examine the behaviour of the unsteady viscous layers that exist on spheroidal particles in axisymmetric flow. The study leads to an approximate expression for the functional form of the force on an arbitrary body in unsteady flow at low Reynolds number.

Related solutions exists for a sphere oscillating along its diameter, see the classic paper by Stokes (1851), and a variety of problems where the stream-lines are straight and there is no pressure gradient or normal velocity component. The latter include the impulsive motion of infinite cylinders of general cross-section parallel to their axis (Batchelor 1954; Hasimoto 1955) and the impulsive or oscillatory motion of a wall in its own plane. Although the solutions for the sphere and the infinite-aspect-ratio body exhibit fundamental differences in behaviour there has been no previous study that examines the transition in behaviour of the unsteady viscous layers between these two limits of geometry over the frequency spectrum. The recent paper by Lawrence & Weinbaum (1986) has shown that the force on an oscillating perturbed sphere has a previously unrecognized term whose phase varies with frequency, which for an arbitrary $U(t)$ transforms to a memory integral whose kernel differs from the classic $t^{-\frac{1}{2}}$ behaviour. In the present paper the solutions for an arbitrary spheroid will be presented to elucidate the complete transition in behaviour that occurs as a function of aspect ratio and frequency.

The linearized Navier–Stokes equations differ from the more frequently studied steady Stokes equation in the inclusion of the unsteady inertia term:

$$\rho\frac{\partial \boldsymbol{u}}{\partial t} = -\nabla p + \mu\nabla^2\boldsymbol{u}, \quad \nabla\cdot\boldsymbol{u} = 0. \tag{1}$$

The well-known solution to (1) for the shear stress on an oscillating plane wall is

$$\mu\frac{\partial u}{\partial y}(0) = \mathrm{Re}\left\{-\frac{\mu}{\delta}\,\mathrm{e}^{-\mathrm{i}\pi/4}\,U\,\mathrm{e}^{-\mathrm{i}\omega t}\right\}, \tag{2}$$

while the solution for the hydrodynamic force on an oscillating sphere is given by

$$F = \mathrm{Re}\left\{-6\pi\mu a\left[1+\frac{a}{\delta}\,\mathrm{e}^{-\mathrm{i}\pi/4}+\frac{1}{9}\left(\frac{a}{\delta}\right)^2\mathrm{e}^{-\mathrm{i}\pi/2}\right]U\,\mathrm{e}^{-\mathrm{i}\omega t}\right\}. \tag{3}$$

Here μ is the fluid viscosity, a is the sphere radius, U is the peak velocity and δ is the penetration depth $(\nu/\omega)^{\frac{1}{2}}$, where ω is the frequency of oscillation and ν the kinematic viscosity. δ characterizes the distance that the centroid of vorticity diffuses normal to the wall during a single oscillation. A critical dimensionless parameter which determines the physics of the solution in (3) is a/δ. At low frequencies, when a/δ is small, the force on the sphere is dominated by the first or steady Stokes drag term while the second term, which is $\frac{1}{4}\pi$ out of phase with the velocity, is a correction due to the unsteady viscous layer that envelopes the sphere. The phase difference arises from the fact that the inner regions of the layer are in phase with the velocity of the body, whereas the outer inviscid regions are $\frac{1}{2}\pi$ out of phase. The total stress correction at the surface comes from two contributions: an unsteady shearing stress and a displacement effect on the outer inviscid flow which modifies the normal stress or pressure field. The relative importance of these two contributions changes with frequency. At low frequency one can show using the theory of matched asymptotic expansions that the correction is due primarily to an alteration of the inviscid far field which lies beyond δ. The intriguing feature is that the wall stress in (2) has

exactly the same phase as the correction term in (3), although it does not depend on a displacement of the outer flow since, for the plane wall, there is no normal velocity component.

The behaviour of (3) in the high-frequency or boundary-layer limit where $a/\delta \gg 1$ is easily seen by rewriting it in the form

$$F = \mathrm{Re}\left\{-\tfrac{2}{3}\pi\rho a^3\omega\, \mathrm{e}^{-\mathrm{i}\pi/2}\left[1+9\frac{\delta}{a}\mathrm{e}^{\mathrm{i}\pi/4}+9\left(\frac{\delta}{a}\right)^2\mathrm{e}^{\mathrm{i}\pi/2}\right]U\,\mathrm{e}^{-\mathrm{i}\omega t}\right\}, \tag{4}$$

where it is apparent that the unsteady damping force is a first-order correction of $O(\delta/a)$ to the virtual mass force. Batchelor (1967) has shown that for a sphere, two-thirds of the real part of this term comes from the viscous stress whereas the remainder is due to the displacement effect on the outer inviscid flow. This distribution between the viscous stress and displacement contribution depends strongly on aspect ratio and can be determined for other body geometries only in the boundary-layer limit in which the viscous-stress term can be calculated independently by applying (2) locally and integrating over the surface. Two important observations can be made in relation to (3) and (4). The first is that the phase of the unsteady viscous-damping term is the same throughout the frequency spectrum although the relative contributions of the viscous stress and displacement effects change with frequency. The second is that the relative importance of the steady and unsteady damping forces changes markedly as the aspect ratio increases. It will be convenient to introduce the complex frequency parameter $\lambda^2 = -\mathrm{i}\omega a^2/\nu$, where λ is the coefficient of the unsteady viscous-stress term in (3). For a sphere the second term will be the dominant one only for a very limited frequency range defined by $1 < |\lambda| < 9$, whereas for an elongated body the force component with phase $\frac{1}{4}\pi$ must become increasingly important over a wider range of the frequency spectrum since to leading order the surface stress must eventually approach (2) with corrections for end effects and transverse curvature. This prediction has significant implications for the interaction between elongated particles in colloidal suspensions where the unsteady viscous interaction force has in the large been neglected. For reasons that will be discussed in the concluding comments this is a reasonable approximation for spheres but may be invalid for high-aspect-ratio spheroids.

Crucial insights into the first observation made above have recently been obtained from the solution to (1) for a perturbed sphere in the form of a spheroid (figure 1) with semi-axes related by $a = b(1+\epsilon)$, where ϵ is a perturbation parameter (Lawrence & Weinbaum 1986). It can be shown that for this near sphere the total hydrodynamic force takes the form

$$F = \mathrm{Re}\{-6\pi\mu a[F_\mathrm{s} + B\lambda + m_\mathrm{a}\lambda^2 + \phi(\lambda,\epsilon)]\,U\,\mathrm{e}^{-\mathrm{i}\omega t}\}, \tag{5a}$$

where $\lambda^2 = -\mathrm{i}\omega a^2/\nu$ as above and

$$F_\mathrm{s} = 1 - \tfrac{1}{5}\epsilon + \tfrac{37}{175}\epsilon^2 + O(\epsilon^3), \tag{5b}$$

$$B = 1 - \tfrac{2}{5}\epsilon + \tfrac{81}{175}\epsilon^2 + O(\epsilon^3), \tag{5c}$$

$$m_\mathrm{a} = \tfrac{1}{9}(1 + \tfrac{1}{5}\epsilon - \tfrac{26}{175}\epsilon^2) + O(\epsilon^3), \tag{5d}$$

$$\phi(\lambda,\epsilon) = \frac{8\epsilon^2}{175}\left(\frac{\lambda^2}{3+3\lambda+\lambda^2}\right) + O(\epsilon^3). \tag{5e}$$

The coefficients F_s and m_a are identical with the respective limits of Sampson's (1891) solution (Happel & Brenner 1965) and Green's solution (1833) for a slightly oblate or

prolate spheroid. The B-term with $\frac{1}{4}\pi$ phase can be shown to be at $O(\epsilon^2)$ either the first-order correction for the unsteady viscous stress at low frequency or the first-order correction to the virtual mass force for the thin viscous boundary layer at high frequency. The solution in the low-frequency limit is a special case of the more general formula

$$F = -6\pi\mu a U\cdot[\boldsymbol{A}+\lambda\boldsymbol{A}\cdot\boldsymbol{A}+O(\lambda^2)] \tag{6}$$

derived by Lawrence (1988) for an arbitrary body performing slow harmonic oscillations in which $\boldsymbol{A}$ is the frictional resistance tensor for steady Stokes flow. At $O(\epsilon^2)$ one can show that the asymptotic formulas for the coefficient B differ in the high- and low-frequency limits. This difference is borne out by the asymptotic solutions at high and low frequency for a spheroid of arbitrary aspect ratio presented in §3, suggesting that a modified form of (5) will be necessary for bodies whose aspect ratio is not unity.

The most interesting result embodied in (5) is the presence of a new term coupling frequency and geometry, $\phi(\lambda,\epsilon)$, which has a large phase variation as a function of frequency. In the low-frequency limit $\lambda\to 0, \phi\sim(8\epsilon^2/525)\lambda^2$ and hence this term exhibits a $\frac{1}{2}\pi$ phase shift. This can be interpreted as a second-order correction to the inviscid outer flow at low frequency due to the displacement effect of the inner viscous region. In the high-frequency limit $\phi\sim 8\epsilon^2/175$ and there is no phase shift. This is a second-order viscous correction to the virtual-mass term; it is in phase with velocity and thus equivalent to an additional Stokes-drag term. At intermediate frequencies there is a monotonic variation in phase between these two limiting cases. Although the corrections are small for the slightly oblate spheroid it is clear from these results that the sphere is a special case in which the unsteady shear stress and displacement effects on the inviscid flow combine in such a way that the phase of the unsteady stress term is always $\frac{1}{4}\pi$ ahead of the velocity for all frequencies. This arises from the simple functional form of the solution for the stream function for a sphere in spherical coordinates. The angular dependence of the distribution of vorticity is simply separable, which provides for a spherical displacement body at all frequencies – in the general case, the displacement body is spherical only at low frequency. In the present paper we shall want to generalize (5) to apply to spheroids of any aspect ratio and also propose an approximate functional form for other body shapes.

Another novel aspect of (5) is that it leads to an expression for the force on a near sphere moving with an arbitrary velocity $W(t)$ that has a new memory function in addition to the $t^{-\frac{1}{2}}$ memory function derived by Basset (1888) for the force whose phase is $\frac{1}{4}\pi$ ahead of the velocity. The parameter λ^2 can be viewed as the Laplace-transform variable in the superposition of the solution over all frequencies. The Laplace inversion can be performed analytically and is shown in Lawrence & Weinbaum (1986) to be of the form†

$$\mathscr{F}(t) = -6\pi\mu a\left\{F_s W(t)+\frac{a}{(\nu\pi)^{\frac{1}{2}}}B\int_0^t\frac{\mathrm{d}W}{\mathrm{d}\tau}\frac{\mathrm{d}\tau}{(t-\tau)^{\frac{1}{2}}}+\frac{a^2}{\nu}m_a\frac{\mathrm{d}W}{\mathrm{d}t}+\frac{a}{(\nu\pi)^{\frac{1}{2}}}\int_0^t\frac{\mathrm{d}W}{\mathrm{d}\tau}G(t-\tau)\,\mathrm{d}\tau\right\}, \tag{7a}$$

$$G(t) = \frac{8\epsilon^2}{175}\,\mathrm{Im}\,\{(\tfrac{1}{3}\pi\alpha)^{\frac{1}{2}}\mathrm{e}^{\alpha t}\,\mathrm{erfc}\,(\alpha t)^{\frac{1}{2}}\},\quad \alpha=\tfrac{3}{2}(1+\mathrm{i}\sqrt{3}). \tag{7b}$$

† The factor of 6 was erroneously omitted from the fourth term in the original paper.

The first three terms are the classical Stokes-drag, Basset-force and virtual-mass contributions to the total hydrodynamic force. These are the only force components for a spherical particle in transient motion. The particular form of the memory term in the Basset-force integral occurs only for an unsteady viscous stress which is proportional to λ, that is a force component which is $\frac{1}{4}\pi$ ahead of the velocity and whose amplitude varies as $\omega^{\frac{1}{2}}$. For any non-spherical body there will be a frequency-dependent force whose memory integral depends on the geometry in a more complicated fashion. For a slightly oblate spheroid the memory-function is given by (7*b*). This memory function is bounded as $t \to 0$ and decays as $t^{-\frac{3}{2}}$ for large t. For an arbitrary spheroid the geometry-dependent memory function is much more complicated and does not have a simple closed-form analytic representation. We shall show, however, that a surprisingly good correlation approximation is possible which should prove adequate for most purposes. Both memory integrals will play an increasingly important role for elongated spheroids since the range of frequencies over which the unsteady stress terms dominate in the generalized form of (5) grows as the aspect ratio increases. We shall find that the generalized Basset-force integral term has a dimensionless coefficient of order $|\boldsymbol{A}\cdot\boldsymbol{A}|\,Re^{\frac{1}{2}}$. The memory integral terms will be larger than the Stokes drag term when $|\boldsymbol{A}|\,Re^{\frac{1}{2}} > 1$. This is more likely to occur with slender bodies for which $|A| \sim (b/a)\,[1/(\log b/a)]$.

There have been relatively few fundamental studies of the linearized equation (1) compared with its steady-state counterpart. Tchen (1947) derived the inverse result to (7*a*) for a sphere, giving the velocity in terms of an arbitrary time-dependent externally applied force. Lamb (1932) derived a set of solid spherical harmonics for the unsteady Stokes equations (in addition to his better-known solution of the steady equations). Much of the subsequent work has been based on these major contributions, using the basic spherical (or cylindrical) geometry as a starting point. An exception is the work of Hocquart (1976, 1977*a*) who found solutions for the velocity field caused by a spheroidal particle executing oscillatory rotations about its axis or an equatorial diameter. The main emphasis of this work was to understand Brownian motions, as demonstrated by the subsequent papers (Hocquart 1977*b*; Hocquart & Hinch 1983). In this context, it is the low-frequency regime that is important, so there was no need to evaluate the spheroidal wave functions (which arise as part of the solution) in the general case. Aoi (1955*a*, *b*) tackled the mathematically similar problem of Oseen flow past a spheroid, which also leads to spheroidal wave-function solutions and the work was generalized to include higher-order term by Breach (1961). This work was necessarily limited to small inertial corrections, corresponding to the low-frequency limit. In the present article, we shall find the force on a spheroidal particle of arbitrary aspect ratio oscillating with arbitrary frequency along its axis of symmetry.

The problem under discussion has been considered on at least two previous occasions. Kanwal (1955) formulated the problems for axisymmetric rotational and longitudinal oscillations of spheroids and obtained the form for the stream function in terms of spheroidal wave functions given in §4 below. However, he was not able to perform the calculations necessary to evaluate the force. Subsequently Lai & Mockros (1972) followed the same approach and obtained an approximate form for the force on a spheroid in longitudinal acceleration. They used an expansion of the spheroidal wave functions for small values of the parameter c (or equivalently $|\lambda|$) to obtain the form of the force at low frequency correct to first order in $|\lambda|$. For reasons that are unclear, in their result they retained the added-mass term which arose

naturally from integrating the stress on the surface of the spheroid. This is inconsistent since, as we have seen, the added-mass term is of $O(|\lambda|^2)$. In the notation of the present work, their result is

$$F \sim 6\pi\mu U a[F_s + F_1\lambda + m_a\lambda^2 + O(\lambda^2)] \quad \text{for } |\lambda| \ll 1, \tag{8}$$

where F_1 is the coefficient of the low-frequency correction to the steady Stokes drag F_s and is numerically equal to F_s^2 (Lawrence 1988). If the result (8) were extended to higher order, the coefficient of λ^2 would not be m_a. This can be seen by comparison with the analytical result for near spheres (5) where we see that, for the low-frequency expansion, the coefficient of λ^2 should be $m_a + 8\epsilon^2/525$; for aspect ratios substantially different from unity the error will be much larger. In fact, the result (8) is approximately correct for all frequencies when the aspect ratio is close to unity, as we shall discuss in §7. It corresponds to omitting the term $\lambda\phi(\lambda, b/a)$ from (67) and defining the Basset coefficient to be F_1 instead of the high-frequency coefficient B. Clift, Grace & Weber (1978) summarized the above work and were the first to observe that the low-frequency-correction term F_1 is simply the square of the Stokes drag F_s.

Lai (1973) claims to have obtained exact solutions for the transient motion of circular disks along their axis. However, the results presented correspond to the approximate solution (8). When the approximate result is integrated over frequency, an expression for the time-dependent force is obtained which corresponds to (82) with the last term omitted. The mathematical form of this expression differs from that for a sphere only in the values of the three geometrical coefficients for the added mass, Basset force and Stokes drag. As we shall discuss in §5, even the four-term correlation of the current work loses accuracy for bodies of aspect ratio less than 0.1 and the three-term approximation (8) will be even more deficient. Further caution in the use of these results is warranted because, for a real flow, one would expect to see separation behind the disk, which cannot be predicted by the linear theory.

In the next section, the equations of motion will be formulated in terms of the stream function in spheroidal coordinates. The two dimensionless parameters in the problem may be chosen in different ways depending on mathematical convenience. The results will be presented in §5 in terms of the physically significant parameters which are the streamwise/cross-stream aspect ratio b/a, and the frequency parameter $|\lambda| = a(\omega/\nu)^{\frac{1}{2}}$. For most applications, aspect ratios between 0.1 and 10 may be considered. The three limiting cases $b/a = 0, 1, \infty$ correspond to the disk, sphere and infinite cylinder respectively, but are relatively unimportant; an oscillating disk sheds nonlinear vortices at all but the lowest frequencies, whilst the sphere and cylinder can be treated more effectively in their natural coordinate systems (Stokes 1851; Batchelor 1954). The frequency parameter $|\lambda|$ may be quite large (of order 10 or 100 for a pendulum) but is generally small for microscopic particles.

From a general point of view, one would expect the force on an oscillating body to be an arbitrary function of the two dimensionless parameters $|\lambda|$ and b/a. We can impose constraints on the functional form of the force using knowledge of its limiting behaviour. Asymptotic results for small and large frequencies are derived in §3 and these give a good indication of the general solution. The high-frequency behaviour is known to be the added-mass term $m_a\lambda^2$, whilst the low-frequency behaviour is known to be the quasi-steady Stokes term F_s. Thus, at intermediate frequency, the force is restricted to behaviour between $O(|\lambda^0|)$ and $O(|\lambda^2|)$. It is then to be expected that the force will have similar functional form to the quadratic dependence on λ

observed for a sphere (3). After a representative linear term has been identified, the remaining frequency-dependent and phase-varying term should be small. It proves to be convenient to use the second term at high frequency for the $O(\lambda)$ Basset term; this definition of B thus provides for a self-consistent generalization of the Basset force for non-spherical bodies. In this way the force can be represented as the sum of four contributions, three of which form a quadratic in λ with known closed-form analytic expressions for the geometrical dependence of the coefficients. The fourth term is necessarily more complicated, varying from $O(\lambda)$ at low frequency to $O(1)$ at high frequency. However, it vanishes identically for a sphere and remains small at all frequencies for bodies that have aspect ratio of order unity. The general analytic solution for arbitrary frequency is presented in §4, and all the results are combined in §5. Exact numerical solutions are obtained in the parameter ranges $0.1 < b/a < 10, 0.1 < |\lambda| < 10$.

The graphical results suggest a simple form for a correlation of the fourth term in the force, the other three terms being known exactly. The four-term correlation is accurate in the range $0.1 < b/a < 10$ for all frequencies and reduces to Stokes' result (3) for a sphere. Because three of the terms in the force ar known exactly and the fourth term is relatively small, the four-term representation for the force is highly accurate. An important feature of the correlation is that the inverse transform may be found analytically for an arbitrary spheroid to give the result corresponding to (7) and Basset's result for a sphere. The inverse transform is described in §6. The results are discussed in the concluding section and an extension of the approximate representation is proposed to apply the method to a body of arbitrary shape.

2. Formulation in spheroidal coordinates

We consider the spheroid generated by rotating the ellipse $\varpi^2/a^2 + z^2/b^2 = 1$ about the z-axis as shown in figure 1(*a*). For the time being, we shall restrict consideration to an oblate spheroid, with $b < a$, although it will prove to be simple to extend the results to the prolate case (see §4). We introduce conjugate coordinates of revolution (ξ, η) with $x = \sinh\xi$ and $y = \cos\eta$ defined by

$$z = dxy, \quad \varpi = d(1+x^2)^{\frac{1}{2}}(1-y^2)^{\frac{1}{2}}, \tag{9}$$

where $d = (a^2 - b^2)^{\frac{1}{2}}$ is the radius of the focal circle. The surface of the spheroid is now the coordinate surface $x = x_0$ with

$$x_0^2 = \left[\left(\frac{a}{b}\right)^2 - 1\right]^{-1}, \quad a^2 = d^2(1+x_0^2), \quad b^2 = d^2 x_0^2, \tag{10}$$

and the flow domain is the region $x_0 \leqslant x < \infty, 1 \leqslant y \leqslant 1$.

The spheroid is a solid body which executes oscillations along its axis of symmetry with velocity $U\cos\omega t\, \boldsymbol{i}_z$. If the velocity of the fluid is so small that nonlinear terms may be neglected, the equations of motion are the linearized Navier–Stokes equations (1), also known as the unsteady Stokes equations.

We take the curl of the momentum equation to eliminate the pressure and introduce the stream function Ψ defined in cylindrical coordinates by

$$\boldsymbol{u}\cdot\boldsymbol{i}_\varpi = \frac{1}{\varpi}\Psi_z, \quad \boldsymbol{u}\cdot\boldsymbol{i}_z = -\frac{1}{\varpi}\Psi_\varpi. \tag{11}$$

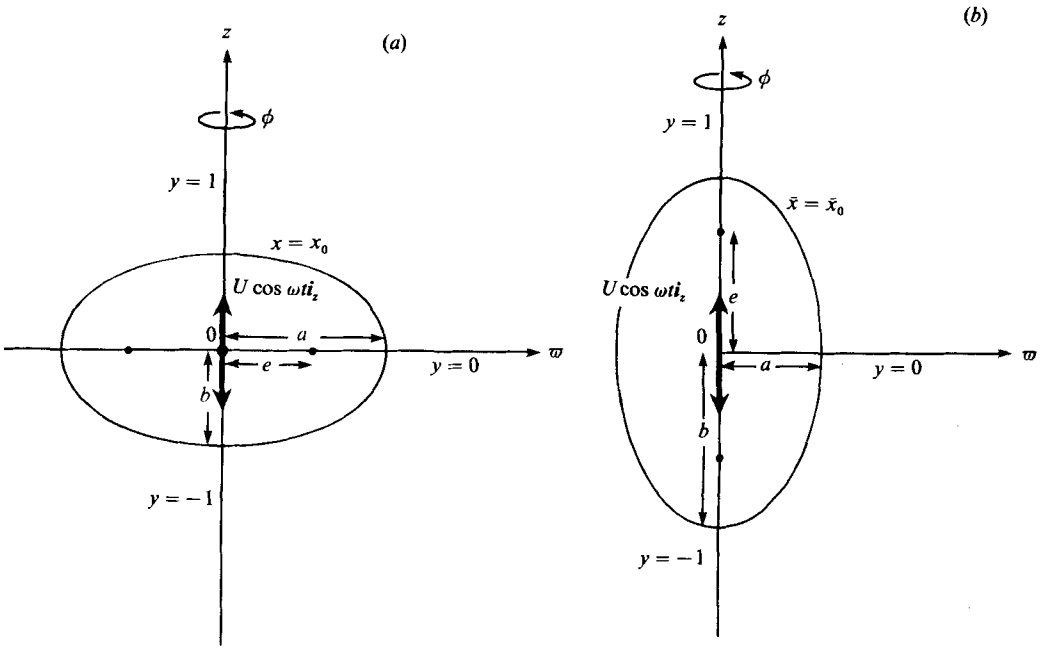

FIGURE 1. The geometry and coordinate system for (*a*) an oblate spheroid, and (*b*) a prolate spheroid.

Then we have the vorticity equation

$$E^4\Psi - \frac{1}{\nu}E^2\Psi_t = 0, \tag{12}$$

where E^2 is the generalized axisymmetric potential operator given in oblate spheroidal coordinates by

$$E^2 = \frac{1}{d^2(x^2+y^2)}\left[(1+x^2)\frac{\partial^2}{\partial x^2} + (1-y^2)\frac{\partial^2}{\partial y^2}\right]. \tag{13}$$

The limiting conditions on the velocity are:

on the body $$\boldsymbol{u} = U\cos\omega t\, \boldsymbol{i}_z, \tag{14a}$$

at infinity $$\boldsymbol{u} \to 0. \tag{14b}$$

The rate of decay of $\boldsymbol{u}$ must be so fast that there are no source terms at infinity. Therefore we need

$$r^2\boldsymbol{u} \to 0 \quad \text{as } r \to \infty, \tag{15}$$

where $r^2 = \varpi^2 + z^2$ is the spherical radius. We also require that there are no singularities in the flow field. (This precludes the limit $x_0 = 0$ in which the body is a disk). The flow is periodic in time, so we may take the stream function to be of the form $\Psi(\varpi, z, t) = \mathrm{Re}\{\psi(\varpi, z)\, e^{-i\omega t}\}$ where ψ may be complex. Then we have

$$E^4\psi + i\frac{\omega}{\nu}E^2\psi = 0, \tag{16}$$

$$\left.\begin{aligned}\psi &= -\tfrac{1}{2}\varpi^2 U = -\tfrac{1}{2}d^2U(1+x_0^2)(1-y^2)\\ \psi_x &= \varpi\varpi_x U = -d^2U(1-y^2)x_0\end{aligned}\right\} \quad \text{on } x = x_0, \tag{17, 18}$$

$$\psi \to 0 \quad \text{as } x \to \infty, \tag{19}$$

$$\psi = 0, \quad \psi_y \text{ is finite}, \quad \text{on } y = \pm 1. \tag{20}$$

There is also symmetry about the plane $y = 0$, so we have $\psi(y) = \psi(-y)$ and $\psi_y = 0$ on $y = 0$. It is worthy of note that (16)–(20) are valid in the coordinate system that is fixed in the body. This accelerated frame of reference has no effect other than the inclusion in the force of a buoyancy-like term which is equal to the acceleration times the mass of the displaced volume of fluid.

We are ultimately interested in the force on the body which is of the form $\mathscr{F}_{\mathrm{H}} = \mathrm{Re}\{F\,\mathrm{e}^{-\mathrm{i}\omega t}\}$. The complex amplitude F is given by Lawrence & Weinbaum (1986) to be

$$F = -\rho \mathrm{i}\omega \left[UV + 4\pi \lim_{r\to\infty} \frac{r^3}{\varpi^2}\psi\right], \tag{21}$$

where $V = \frac{4}{3}\pi a^2 b$ is the volume of the body.

To facilitate the solution, we introduce dimensionless quantities with velocity scale U, lengthscale d, and force scale $\mu U d$ as follows:

$$\psi^* = \frac{\psi}{d^2U}, \quad (\mathrm{E}^2)^* = d^2\mathrm{E}^2, \quad F^* = \frac{F}{\mu U d}, \quad V^* = \frac{V}{d^3} = \tfrac{4}{3}\pi x_0(1+x_0^2). \tag{22}$$

The asterisks will be ignored and the governing equations simplify to

$$\mathrm{E}^4\psi - c^2\mathrm{E}^2\psi = 0, \quad \text{with } c^2 = -\frac{\mathrm{i}\omega d^2}{\nu}, \quad \mathrm{Re}\{c\} > 0 \tag{23}$$

$$\psi = -\tfrac{1}{2}(1+x_0^2)(1-y^2), \quad \psi_x = -x_0(1-y^2) \quad \text{on } x = x_0. \tag{24}$$

Conditions (19) and (20) are unchanged.

The above is a linear boundary-value problem with two parameters x_0 and $|c|$. It is more usual to use the parameters: aspect ratio b/a, frequency parameter $|\lambda| = a(\omega/\nu)^{\frac{1}{2}}$, as well as to use the dimensionless force $F_a^* = F/6\pi\mu U a$. However, this would unnecessarily complicate the equations. After the results are obtained, it is simple to convert them to the more usual parameters by using lengthscale a instead of d in (22).

3. Analytic solutions found via small perturbations

The solution to (19)–(24) is very complex in the general case and will be treated in §4. Valuable insights can first be obtained by examining certain limiting cases which will also be useful for checking the full calculations. Two cases will be considered: (*a*) low frequency, $|c| \ll 1$; and (*b*) high frequency, $|c| \gg 1$. The case of a nearly spherical body, $x_0 \gg 1$, was considered previously (Lawrence & Weinbaum 1986).

3.1. *Low frequency*

At very low frequencies, the flow becomes quasi-steady and so the solution to zero order is that for steady flow past a spheroid first given by Sampson (1891) and discussed by Happel & Brenner (1965) (here we use the dimensionless quantities of §2):

$$\psi_0 = (1-y^2)\{-\tfrac{1}{2}C_1 x + \tfrac{1}{2}C_2[x - (x^2+1)\cot^{-1}x] + C_3(x^2+1)\}, \tag{25}$$

with $$C_1 = \frac{2}{x_0 - (x_0^2-1)\cot^{-1} x_0}, \quad C_2 = \frac{-(x_0^2-1)}{x_0 - (x_0^2-1)\cot^{-1} x_0}, \quad C_3 = 0, \tag{26}$$

and $$F_0 = -4\pi C_1 = \frac{-8\pi}{x_0 - (x_0^2-1)\cot^{-1} x_0}. \tag{27}$$

Lawrence (1988) has shown that the force on a general body at low frequency is given by (6), in which $\boldsymbol{A}$ is the resistance tensor for arbitrary slow motion of the body. For the axisymmetric motion of a spheroid, (6) loses its tensorial nature and the dimensionless force is given by

$$F = -6\pi[A_{\parallel} + cA_{\parallel}^2 + O(c^2)], \tag{28}$$

in which $$A_{\parallel} = -\frac{F_0}{6\pi} = \tfrac{4}{3}[x_0 - (x_0^2-1)\cot^{-1} x_0]^{-1}. \tag{29}$$

The result (28) has been verified directly via asymptotic matching of inner and outer fields by Lawrence (1986) and is in agreement with the first-order low-frequency expansion of Lai & Mockros (1972).

3.2. *High frequency*

When the frequency of oscillation is very high, the flow field will be almost inviscid and the potential-flow solution will be valid everywhere except in a thin boundary layer on the surface of the body. In order to calculate the perturbed stream function, one must compute the boundary-layer velocities and the displacement effect on the external pressure field via matched asymptotic expansions. However, Batchelor (1967) describes a simple method for obtaining the in-phase part of the force, i.e. the damping force, by integrating the dissipation in the boundary layer.

It is clear that the force on the body may be represented in the asymptotic (dimensional) form:

$$F \sim -6\pi\mu U a(\lambda^2)[m_a + \lambda^{-1}B + O(\lambda^{-2})], \tag{30}$$

where m_a is the dimensionless scaled added mass, found from Green (1833):

$$m_a = +\frac{2}{9}\frac{(1+x_0^2)^{\frac{1}{2}}(1 - x_0\cot^{-1} x_0)}{[x_0 - (1+x_0^2)\cot^{-1} x_0]}. \tag{31}$$

Batchelor (1967) gives the in-phase part of the force to be $F_R \cos\omega t$ with

$$\tfrac{1}{2}UF_R = \frac{\mu}{2\delta}\int_{\text{body}} U_s^2 \, dA, \quad \delta = \left(\frac{2\nu}{\omega}\right)^{\frac{1}{2}} \ll a. \tag{32}$$

In (32), U_s is the velocity of the fluid at the surface of a body that is stationary in uniform potential flow at infinity. Batchelor (1967) also gives the stream function for a spheroid moving through stationary inviscid fluid to be

$$\psi = \tfrac{1}{2}Ua^2(1-y^2)\left[\frac{x - (1+x^2)\cot^{-1} x}{x_0 - (1+x_0^2)\cot^{-1} x_0}\right]. \tag{33}$$

To change (33) to the case of the stationary spheroid, we simply subtract a uniform stream, which is a term

$$\tfrac{1}{2}Ua^2\frac{(1+x^2)}{(1+x_0^2)}(1-y^2). \tag{34}$$

The velocity components are

$$\boldsymbol{u}\cdot\boldsymbol{i}_x = -\frac{\psi_y}{a^2}\frac{(1+x_0^2)^{\frac{1}{2}}}{(1+x^2)^{\frac{1}{2}}(x^2+y^2)^{\frac{1}{2}}}, \tag{35a}$$

$$\boldsymbol{u}\cdot\boldsymbol{i}_y = \frac{\psi_x}{a^2}\frac{(1+x_0^2)^{\frac{1}{2}}}{(1-y^2)^{\frac{1}{2}}(x^2+y^2)^{\frac{1}{2}}}, \tag{35b}$$

and the elemental area $\mathrm{d}A$ is given by

$$\mathrm{d}A = 2\pi a^2(1+x_0^2)^{-\frac{1}{2}}(x_0^2+y^2)^{\frac{1}{2}}\,\mathrm{d}y, \tag{36}$$

so

$$F_{\mathrm{R}} = -\frac{2\pi\mu}{U}\left(\frac{\omega}{2\nu}\right)^{\frac{1}{2}}\int_{-1}^{1}\frac{1}{d^2}\psi_x^2\frac{(1+x_0^2)^{\frac{1}{2}}\,\mathrm{d}y}{(x^2+y_0^2)^{\frac{1}{2}}(1-y^2)}. \tag{37}$$

Now (33), (34) and (37) are combined to give

$$F_{\mathrm{R}} = -2\pi\mu U a^2\left(\frac{\omega}{2\nu}\right)^{\frac{1}{2}}(1+x_0^2)^{-\frac{1}{2}}\left[\frac{(1+x_0^2)(1-x_0\cot^{-1}x_0)}{x_0-(1+x_0^2)\cot^{-1}x_0}-x_0\right]^2 \times\int_{-1}^{1}\frac{(1-y^2)}{(x_0^2+y^2)^{\frac{1}{2}}}\,\mathrm{d}y. \tag{38}$$

The integral in (38) is evaluated with the help of Gradshteyn & Ryzhik (1980) to give

$$F_{\mathrm{R}} = -2\pi\mu U a^2\left(\frac{\omega}{2\nu}\right)^{\frac{1}{2}}(1+x_0^2)^{-\frac{1}{2}}\left[\frac{(1+x_0^2)(1-x_0\cot^{-1}x_0)}{(x_0-(1+x_0^2)\cot^{-1}x_0)}-x_0\right]^2. \times\left[(2+x_0^2)\sinh^{-1}\frac{1}{x_0}-(1+x_0^2)^{\frac{1}{2}}\right] \tag{39}$$

and

$$B = -\frac{\sqrt{2}}{|\lambda|}\frac{F_{\mathrm{R}}}{6\pi\mu U a} = \tfrac{1}{3}(1+x_0^2)\left[\frac{x_0}{(1+x_0^2)^{\frac{1}{2}}}-\tfrac{9}{2}m_{\mathrm{a}}\right]^2 \times\left[(2+x_0^2)(1+x_0^2)^{-\frac{1}{2}}\sinh^{-1}\left(\frac{1}{x_0}\right)-1\right]. \tag{40}$$

Clearly the first-order correction B given by (40) is not the same as that obtained for low frequencies $A_{\parallel}^2$ given by (29). Hence, only for a sphere will the first-order corrections for the frequency dependence of the force in the high- and low-frequency limits be the same. Result (3) is a remarkably simple special case.

4. Full solution in spheroidal harmonics

The governing equation (23) may be factored to give

$$\mathrm{E}^2(\mathrm{E}^2-c^2)\psi = 0. \tag{41}$$

This in turn has a solution made up of two parts:

$$\psi = \psi^{\mathrm{P}}+\psi^{\mathrm{D}}. \tag{42}$$

The first part, ψ^{P}, is a potential function and must satisfy the equation

$$\mathrm{E}^2\psi^{\mathrm{P}} = 0. \tag{43}$$

The second part, ψ^{D}, is a diffusive function and satisfies

$$(\mathrm{E}^2-c^2)\,\psi^{\mathrm{D}}=0. \tag{44}$$

The inhomogeneous terms generated may be absorbed in ψ^{P}. It is simpler to treat the two components separately as far as is possible and combine them at the end. The following solution parallels those of Kanwal (1955) and Lai & Mockros (1972), although the choice of representation differs somewhat. For this reason, only a brief derivation will be given. Details may be found in Lawrence (1986).

The two terms ψ^{P} and ψ^{D} are separately required to satisfy the homogeneous boundary conditions which guarantees the same of ψ itself. The resulting solutions are

$$\psi^{\mathrm{P}}=(1-y^2)^{\frac{1}{2}}(1+x^2)^{\frac{1}{2}}\sum_{n=1}^{\infty}{}'\,A_n\,P_n^1(y)\,Q_n^1(\mathrm{i}x), \tag{45}$$

$$\psi^{\mathrm{D}}=(1-y^2)^{\frac{1}{2}}(1+x^2)^{\frac{1}{2}}\sum_{n=1}^{\infty}{}'\,B_n\,S_{1n}(c,y)\,R_{1n}^{(3)}(c,\mathrm{i}x). \tag{46}$$

Fore-and-aft symmetry requires that the arbitrary constants A_n and B_n are zero for even values of n, and Σ' indicates that only alternate values of n are included in the sum. The functions P_n^1, Q_n^1 are associated Legendre functions of the first and second kind of order one. The functions S_{1n} are the *prolate* angle spheroidal wave functions of the first kind of order one, while the functions $R_{1n}^{(3)}$ are the radial spheroidal wave functions of the third kind of order one (Flammer 1957; Stratton *et al.* 1941; Chu & Stratton 1941).

Before we apply the inhomogeneous conditions (24), we must sum the two components of the solution from (45) and (46). The stream function is

$$\psi=(1-y^2)^{\frac{1}{2}}(1+x^2)^{\frac{1}{2}}\sum_{n=1}^{\infty}{}'\,[A_n\,P_n^1(y)\,Q_n^1(\mathrm{i}x)+B_n\,S_{1n}(c,y)\,R_{1n}^{(3)}(c,\mathrm{i}x)]. \tag{47}$$

This satisfies the requirements of symmetry, evanescence at infinity and regularity at the poles. The coefficients A_n and B_n are to be determined from (24), which gives

$$\sum_{n=1}^{\infty}{}'\,[A_n\,P_n^1(y)\,Q_n^1(\mathrm{i}x_0)+B_n\,S_{1n}(c,y)\,R_{1n}^{(3)}(c,\mathrm{i}x_0)]=-\tfrac{1}{2}(1+x_0^2)^{\frac{1}{2}}(1-y^2)^{\frac{1}{2}}, \tag{48a}$$

$$\sum_{n=1}^{\infty}{}'\,[A_n\,P_n^1(y)\,\mathrm{D}Q_n^1(\mathrm{i}x_0)+B_n\,S_{1n}(c,y)\,\mathrm{D}R_{1n}^{(3)}(c,\mathrm{i}x_0)]=-x_0(1-y^2)^{\frac{1}{2}}. \tag{48b}$$

The differential operator D is defined by

$$\mathrm{D}f(\chi)=\frac{\mathrm{d}}{\mathrm{d}\chi}(\chi^2-1)^{\frac{1}{2}}f(\chi), \tag{49a}$$

so

$$\mathrm{D}f(\mathrm{i}x)=\frac{\mathrm{d}}{\mathrm{d}x}(x^2+1)^{\frac{1}{2}}f(\mathrm{i}x). \tag{49b}$$

At this point, it is convenient to note some of the properties of the functions $P_n^1(y)$ and $S_{1n}(c,y)$. Abramowitz & Stegun (1965) give the definitions

$$P_n^1(y)=-(1-y^2)^{\frac{1}{2}}\frac{\mathrm{d}}{\mathrm{d}y}P_n(y), \tag{50}$$

$$P_1(y)=y,\quad P_2(y)=\tfrac{1}{2}(3y^2-1),\ \text{etc.} \tag{51}$$

So we can determine

$$P_1^1(y) = -(1-y^2)^{\frac{1}{2}}, \quad P_2^1(y) = -3y(1-y^2)^{\frac{1}{2}}, \text{ etc.} \tag{52}$$

The orthogonality relation

$$\int_{-1}^{1} P_m^1(y)\, P_n^1(y)\, \mathrm{d}y = \delta_{mn} \frac{2n(n+1)}{2n+1} \tag{53}$$

and the expansion for n odd†

$$S_{1n}(c, y) = \sum_{0}^{\infty}{}' d_r^{1n}(c)\, P_{1+r}^1(y) \tag{54}$$

are used to determine

$$\int_{-1}^{1} P_m^1(y)\, S_{1n}(c, y)\, \mathrm{d}y = d_{m-1}^{1n}(c) \frac{2m(m+1)}{2m-1} \tag{55}$$

and, finally

$$\int_{-1}^{1} P_m^1(y)\, (1-y^2)^{\frac{1}{2}} = -\int_{-1}^{1} P_m^1(y)\, P_1^1(y)\, \mathrm{d}y = -\tfrac{4}{3}\delta_{m1}. \tag{56}$$

Now we multiply (48) by $P_m^1(y)$ and integrate from $y = -1$ to $y = 1$, making use of the orthogonality relations (53)–(56). This gives

$$A_m\, Q_m^1(\mathrm{i}x_0) \frac{2m(m+1)}{2m+1} + \sum_{n=1}^{\infty}{}' B_n\, R_{1n}^{(3)}(c, \mathrm{i}x_0)\, d_{m-1}^{1n}(c) \frac{2m(m+1)}{2m+1} = \frac{2}{3}(1+x_0^2)^{\frac{1}{2}} \delta_{1m}, \tag{57a}$$

$$A_m\, \mathrm{D}Q_m^1(\mathrm{i}x_0) \frac{2m(m+1)}{2m+1} + \sum_{n=1}^{\infty}{}' B_n\, \mathrm{D}R_{1n}^{(3)}(c, \mathrm{i}x_0)\, d_{m-1}^{1n}(c) \frac{2m(m+1)}{2m+1} = \frac{4}{3} x_0\, \delta_{1m}. \tag{57b}$$

We define $\bar{B}_n = B_n\, R_{1n}^{(3)}(c, \mathrm{i}x_0)$ and rearrange (57) to get

$$A_m + \sum_{n=1}^{\infty}{}' \bar{B}_n\, d_{m-1}^{1n}(c)/Q_m^1(\mathrm{i}x_0) = \delta_{1m}[\tfrac{1}{2}(1+x_0^2)^{\frac{1}{2}}/Q_m^1(\mathrm{i}x_0)], \tag{58a}$$

$$A_m + \sum_{n=1}^{\infty}{}' \bar{B}_n\, d_{m-1}^{1n}(c) \frac{\mathrm{D}R_{1n}^{(3)}(c, \mathrm{i}x_0)}{R_{1n}^{(3)}(c, \mathrm{i}x_0)\, \mathrm{D}Q_m^1(\mathrm{i}x_0)} = \delta_{1m}[x_0/\mathrm{D}Q_m^1(\mathrm{i}x_0)]. \tag{58b}$$

Equations (58) represent a pair of coupled infinite systems of linear equations for the coefficients A_n and $\bar{B}_n$, from which A_n can easily be eliminated. They may be solved by truncation and matrix inversion. The force is found from (21), so we need to obtain $\lim_{r\to\infty}(r^3/\varpi^2)\psi$. Flammer (1957) indicates that the terms of ψ^{D} decay exponentially in the far field, whereas ψ^{P} yields the dominant term (Magnus, Oberhettinger & Soni 1966),

$$\psi \sim (1-y^2)^{\frac{1}{2}}(1+x^2)^{\frac{1}{2}} A_1\, P_1^1(y)\, Q_1^1(\mathrm{i}x) \sim -(1-y^2)^{\frac{2}{3}} A_1\, x^{-1}. \tag{59}$$

so

$$\lim_{r\to\infty} \frac{r^3}{\varpi^2}\psi = \lim_{x\to\infty} \frac{x^3}{x^2(1-y^2)}\psi = -\tfrac{2}{3}A_1. \tag{60}$$

† The $d_r^{1n}(c)$ are determined by a lengthy procedure which is described by Flammer (1957) and Lawrence (1986).

Finally we have

$$F = \tfrac{4}{3}\pi c^2[x_0(1+x_0^2)-2A_1]. \tag{61}$$

Thus the force on the spheroid depends only on the first coefficient A_1. However, the value of A_1 depends on all the coefficients whose values must be found by solving (58) simultaneously. The details of this and other calculations are given by Lawrence (1986).

4.1. *Prolate spheroid*

The prolate spheroid is a simple extension of the oblate spheroid and the problem can be organized so as to generate exactly the same equations and the same result for the force. The geometry is as shown in figure 1(*b*) with $b > a$ and $e^2 = b^2-a^2$. The coordinate transformation is slightly different in this case:

$$z = e\bar{x}y, \quad \varpi = e(\bar{x}^2-1)^{\frac{1}{2}}(1-y^2)^{\frac{1}{2}}. \tag{62}$$

The surface coordinate is $\bar{x}_0 = b/e$, with $a/e = (\bar{x}_0^2-1)^{\frac{1}{2}}$.

The above quantities can be made the same as for an oblate spheroid by using imaginary values of d and x. We let $d = ie$ and $x = -i\bar{x}$, then the problem reduces identically to that for an oblate spheroid. The only difference is that some of the parameters are imaginary.

5. Results and discussion

Several different lengthscales have been used in the preceding sections, so we must first unify the results. The most important lengthscale is a, the radius perpendicular to the motion, and this will be used from now on. We shall use the most appropriate force scale, which is the Stokes drag on a sphere, $6\pi\mu Ua$. The frequency parameter to be used as $\lambda = (1-i)\,a\,(\omega/2\nu)^{\frac{1}{2}}$ or $|\lambda| = a\,(\omega/\nu)^{\frac{1}{2}}$.

The results of the full calculation are plotted as solid lines in figure 2. As can be seen, the results are qualitatively similar to those for a sphere, $b/a = 1$. At low frequencies, the real part of the force dominates and is almost independent of $|\lambda|$; this is the quasi-steady Stokes drag. The imaginary part of the force is small and linear with $|\lambda|$, representing a slight phase shift. At high frequency, the imginary part of the force varies with $|\lambda|^2$ and is dominant; thus the phase is 90°. The real part of the force is important because it results in energy dissipation which, for example, accounts for the damping of an oscillating pendulum. It can be seen that the change in the nature of the force from quasi-steady Stokes flow to near potential flow occurs as $|\lambda|$ changes from about 0.1 to about 100. Accurate numerical results were obtained for oblate spheroids for $|\lambda| < 10$ and for prolate spheroids for $|\lambda|\,b/a < 10$. The asymptotic result of §3.2 may be regarded as accurate for $|\lambda| > 100$, so there remains a gap in which the results are not known accurately. The broken lines of figure 2 represent a correlation based on a 'patching' of the two asymptotic solutions of §§3.1 and 3.2 using an analytic approximation with numerical coefficients determined from the full solution. The derivation of this correlation will be described below.

The asymptotic results may be summarized as

$$-F \sim F_s + F_1\lambda + O(\lambda^2), \quad |\lambda| \ll 1,$$

$$-F \sim m_a\lambda^2 + B\lambda + O(1), \quad |\lambda| \gg 1,$$

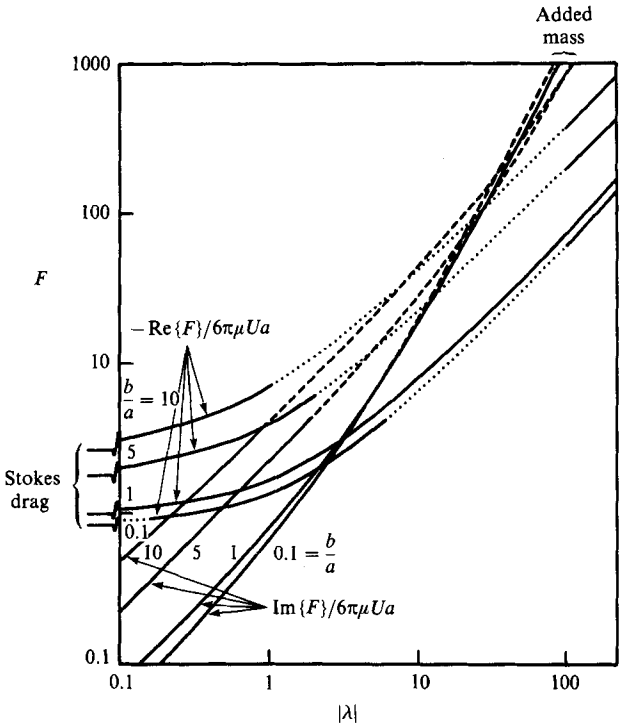

FIGURE 2. The force on an oscillating spheroid as a function of b/a and $|\lambda|$: ——, full calculation; ....., real part of correlation; – – –, imaginary part of correlation.

with

$$F_s = A_{\parallel} = \tfrac{4}{3}[x_0 - (x_0^2 - 1)\coth^{-1} x_0]^{-1}, \tag{63}$$

$$F_1 = A_{\parallel}^2, \tag{64}$$

$$m_a = \tfrac{2}{9}(1+x_0^2)^{\frac{1}{2}} \frac{1 - x_0 \coth^{-1} x_0}{x_0 - (1+x_0^2)\coth^{-1} x_0}, \tag{65}$$

$$B = \frac{1}{3}\left[\frac{x_0}{(1+x_0^2)^{\frac{1}{2}}} - \tfrac{9}{2}m_a\right]^2 (1+x_0^2)\left[1 - (2+x_0^2)(1+x_0^2)^{-\frac{1}{2}} \sinh^{-1}\frac{1}{x_0}\right]. \tag{66}$$

Here, F_s is the Stokes drag correction factor, m_a is the scaled added mass, and F_1 and B are the first-order corrections at low and high frequency. B may be identified as the Basset coefficient for the spheroid. These coefficients are shown in figure 3 where asymptotic components of the force are plotted as functions of the aspect ratio; for the sake of comparison a value of $|\lambda| = 10$ is used. The important feature is the touching of the curves representing the low- and high-frequency first-order corrections at $b/a = 1$. As predicted in Lawrence & Weinbaum (1986), these curves have the same slope and curvature at $b/a = 1$ and they remain close to each other in the range $0.1 < b/a < 10$. It seems reasonable then to represent the force in a way consistent with the results of Lawrence & Weinbaum (1986), equation (5):

$$-F = F_s + B\lambda + m_a\lambda^2 + \lambda\phi\left(\lambda, \frac{b}{a}\right). \tag{67}$$

The remainder term, $\phi(\lambda, b/a)$ will be a complicated function which for low-frequency asymptotes to $(F_1 - B)$ and for high frequency is $O(\lambda^{-1})$. For aspect ratios of order unity, B and F_1 are very close, so ϕ should always be a small contribution to the force.

Using (67) for the definition, $\phi(\lambda, b/a)$ can be calculated from the exact results as far as they are known, and some examples are shown in figure 4 (a–f). For clarity, we have plotted the real and imaginary parts of the function

$$\Phi = \frac{\lambda}{|\lambda|}\phi\left(\lambda, \frac{b}{a}\right), \tag{68}$$

In this way, the phase variation of the result can be seen as well as the amplitude variation. We see that for low frequency, both real and imaginary parts asymptote to $(F_1 - B)/\sqrt{2}$, leading to a phase of $\frac{1}{4}\pi$. At high frequency, both parts asymptote to zero, but the real part does so more slowly, so that the phase will be zero.

These figures suggest that $\phi(\lambda, b/a)$ changes smoothly from $(F_1 - B)$ to zero as the frequency increases, but takes on complex values. The imaginary part of Φ changes at slightly lower frequency. There is a slight overshoot, which is more apparent for aspect ratios closer to unity since F_1 and B are then closer to each other and the scale is greatly magnified. The dotted lines in figure 4 are simply scaled versions of the hyperbolic tangent function which will be used as an approximation for $\phi(\lambda, b/a)$. This approximation is given by

$$\phi\left(\lambda, \frac{b}{a}\right) \approx \tfrac{1}{2}(F_1 - B)\{1 - \tanh[\alpha(\log\lambda - \log\lambda_0)]\}. \tag{69}$$

The form of (69) is reasonable in view of the shape of the curves in figure 4 (a–f) and the fact that F_1 and B are quite close. Equation (69) can be simplified since

$$\tanh[\alpha(\log\lambda - \log\lambda_0)] = \frac{\left(\frac{\lambda}{\lambda_0}\right)^{\alpha} - \left(\frac{\lambda}{\lambda_0}\right)^{-\alpha}}{\left(\frac{\lambda}{\lambda_0}\right)^{\alpha} + \left(\frac{\lambda}{\lambda_0}\right)^{-\alpha}}, \tag{70}$$

so we have

$$\phi\left(\lambda, \frac{b}{a}\right) \approx \frac{F_1 - B}{1 + \left(\frac{\lambda}{\lambda_0}\right)^{2\alpha}}. \tag{71}$$

By a fortunate coincidence, this form of $\phi(\lambda, b/a)$ has the same type of phase shift as the exact solution, as can be observed in figure 4, where the approximation (71) is shown dotted. Suitable values of α and λ_0 have been obtained from the exact solution, i.e. the solid lines of figure 4, in the following way.

When $|\lambda| = \lambda_0$ and $\lambda = \lambda_0 e^{i\pi/4}$, (69) simplifies since

$$\tanh[\alpha(\log\lambda - \log\lambda_0)] = \tanh[\alpha \log(e^{-i\pi/4})] = -i \tan\tfrac{1}{4}\alpha\pi. \tag{72}$$

So we have

$$\phi\left(\lambda_0 e^{-i\pi/4}, \frac{b}{a}\right) \approx \tfrac{1}{2}(F_1 - B)[1 + i \tan\tfrac{1}{4}\alpha\pi]. \tag{73}$$

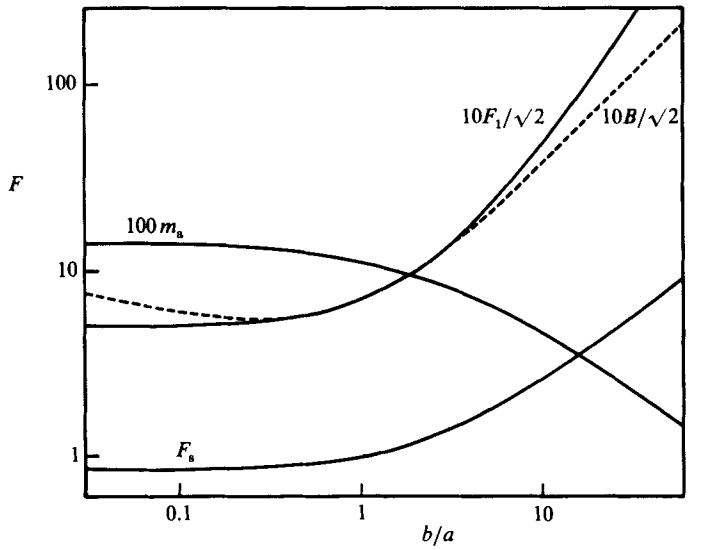

FIGURE 3. Asymptotic components of the force as a function of aspect ratio (nominal value of $|\lambda| = 10$ used for comparison).

Thus in figure 4 when $|\lambda| = \lambda_0$,

$$\mathrm{Re}\{\Phi\} \approx \frac{1}{2\sqrt{2}}(F_1 - B)(1 - \tan\tfrac{1}{4}\alpha\pi) \tag{74}$$

and

$$-\mathrm{Im}\{\Phi\} \approx \frac{1}{2\sqrt{2}}(F_1 - B)(1 + \tan\tfrac{1}{4}\alpha\pi). \tag{75}$$

Thus, λ_0 is the value of $|\lambda|$ where the two curves are equidistant from the centreline $\Phi = \frac{1}{2}(F_1 - B)/\sqrt{2}$, and α is found from

$$\alpha = \frac{4}{\pi}\tan^{-1}\left[\frac{-\mathrm{Im}\{\Phi\} - \mathrm{Re}\{\Phi\}}{(F_1 - B)\sqrt{2}}\right]. \tag{76}$$

The values obtained are displayed in table 1.

At this point, it is convenient to rewrite (67) as

$$-F \approx F_s + B\lambda + m_a\lambda^2 + \left[\frac{F_1 - B}{1 + \left(\dfrac{\lambda}{\lambda_0}\right)^{2\alpha}}\right]\lambda. \tag{77}$$

The approximations to $\phi(\lambda, b/a)$ derived from table 1 and (71) are shown as dotted lines in figure 4, and the corresponding force (77) is shown as broken lines in figure 2.

The least-accurate behaviour of the correlation is at intermediate frequencies and large aspect ratios. From figures 2 and 4(f) we see that with $b/a = 10$ and $|\lambda| = 0.1$, the discrepancy in $\mathrm{Im}\{F\}$ is about 0.5%; the largest error in $\mathrm{Re}\{F\}$ is 0.1% at $|\lambda| = 0.5$. The accuracy of this approximate representation is extraordinary considering the complicated nature of the exact calculation and the simple form of the correlation (77). In addition, a very useful property of the correlation is that (77)

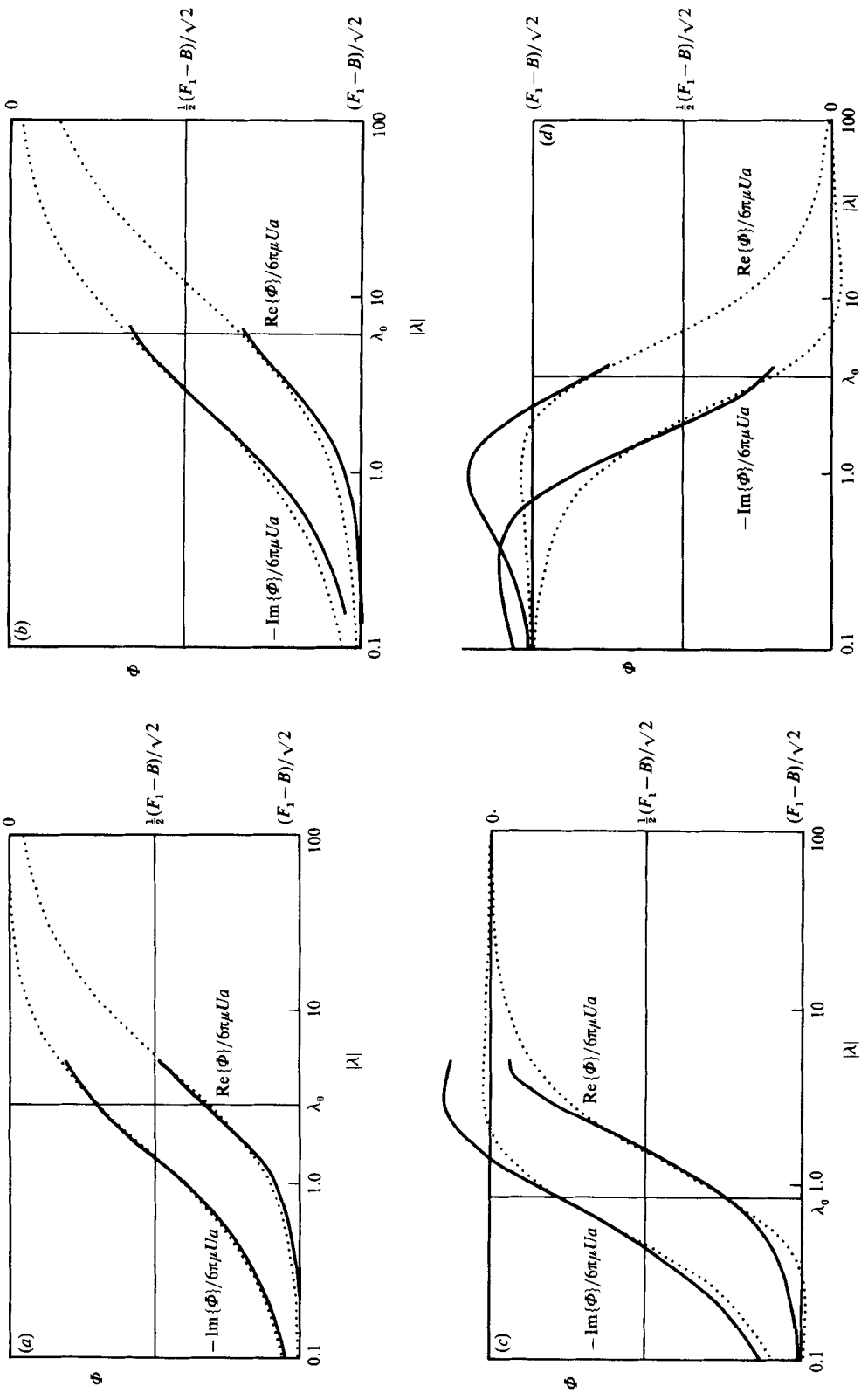
(a)
(b)
(c)
(d)
Φ
|λ|
λ0
0.1
1.0
10
100
0
0.
½(F1 − B)/√2
(F1 − B)/√2
Re{Φ}/6πμUa
−Im{Φ}/6πμUa

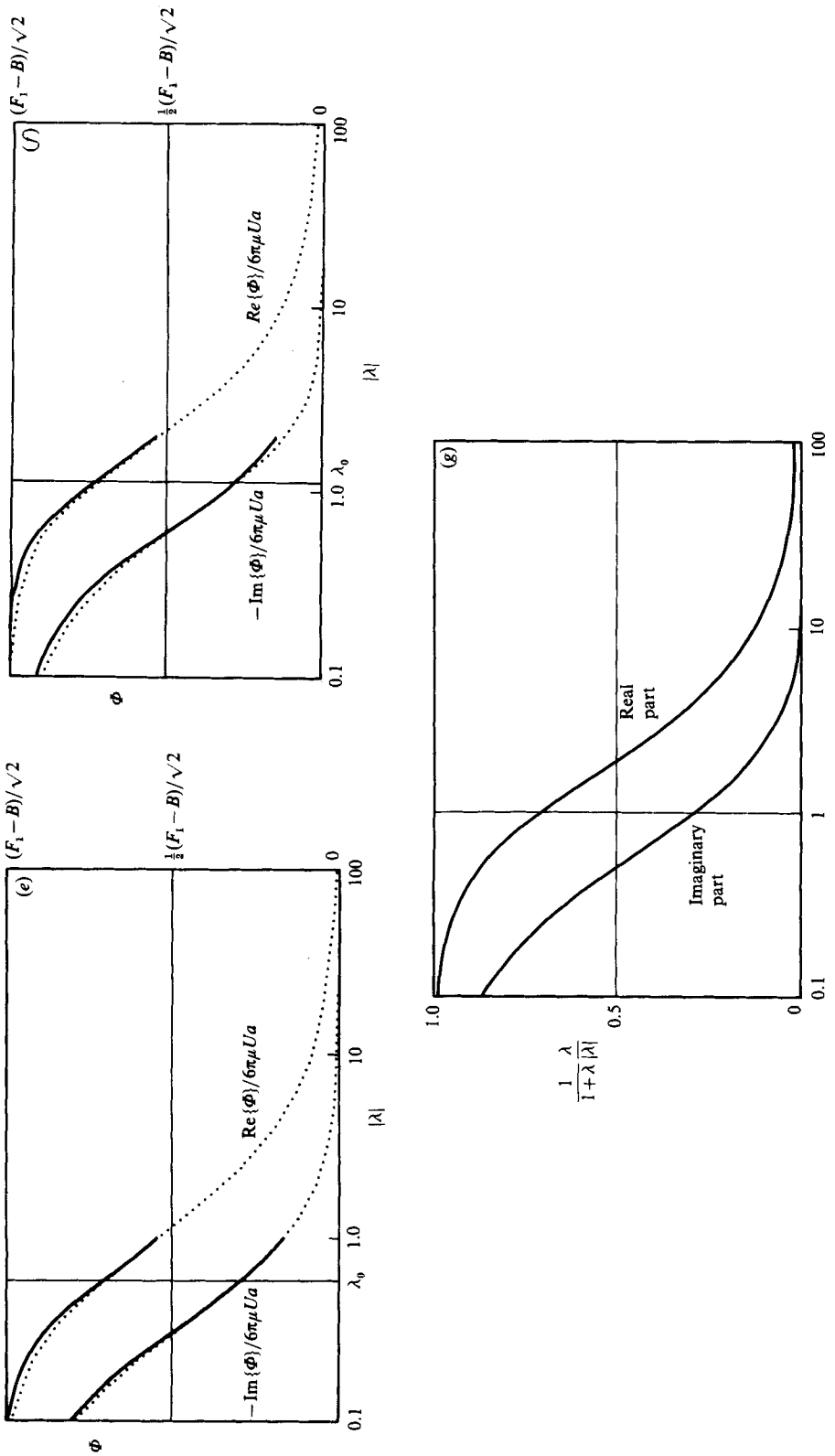

FIGURE 4. The real and imaginary components of the phase-varying coefficient, $\Phi = \phi(\lambda, b/a)\,\lambda/|\lambda|$ as a function of $|\lambda|$: ....., correlation; ——, full calculation. (*a*) $b/a = 0.1$; (*b*) 0.2; (*c*) 0.5; (*d*) 2; (*e*) 5; (*f*) 10; (*g*) crude approximation (94), $\alpha = 0.5, \lambda_0 = 1$.

b/a	0.1	0.2	0.5	1	2	5	10
λ_0	6.07	2.86	0.84	—	3.60	1.12	0.59
α	0.394	0.464	0.636	—	0.687	0.543	0.494

TABLE 1. Values of λ_0 and α for the correlation equation

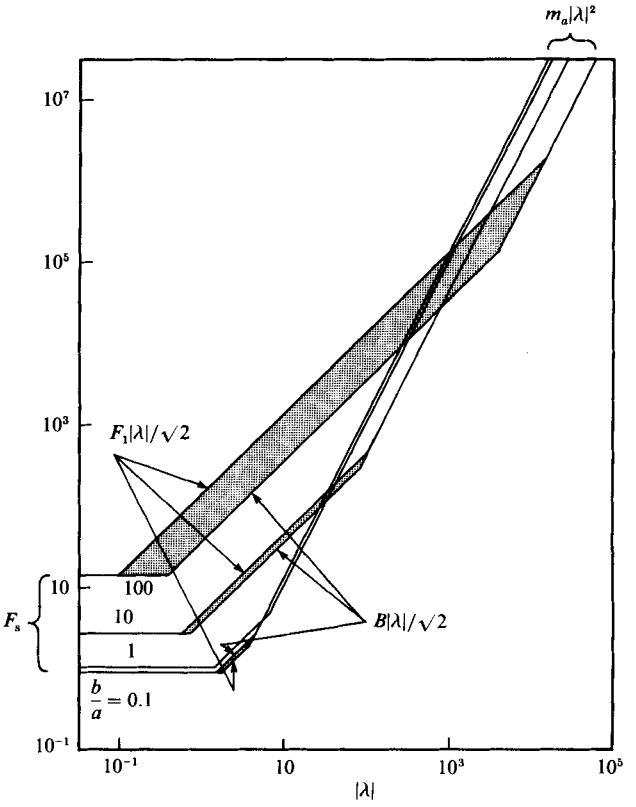

FIGURE 5. Asymptotes of the force as a function of $|\lambda|$ for different aspect ratios.

may be integrated over all frequencies to provide an inverse Laplace transform of the problem, i.e. we can find the transient force for an arbitrary time-dependent velocity, and this will be done in the next section.

Another interesting feature of the results may be observed in figure 3. We can now regard the difference between the two touching curves for the linear corrections as representative of the phase-varying force $\phi(\lambda, b/a)$. When the aspect ratio is large, we see that the added mass is small, since the body is 'streamlined', whereas the Stokes drag and Basset force increase with the length of the body. We can conclude, therefore, that for long bodies at moderately high frequencies the Basset force and phase-varying force are dominant. These considerations are illustrated in figure 5 where the asymptotes for the forces are shown as functions of frequency for a few aspect ratios. Clearly for a body with aspect ratio 100, the Basset force and phase-varying force dominate over the range $1 < |\lambda| < 1000$.

The above discussion leads us to expect that long bodies exhibit three distinct types of behaviour depending on the frequency of oscillation. At very low frequency,

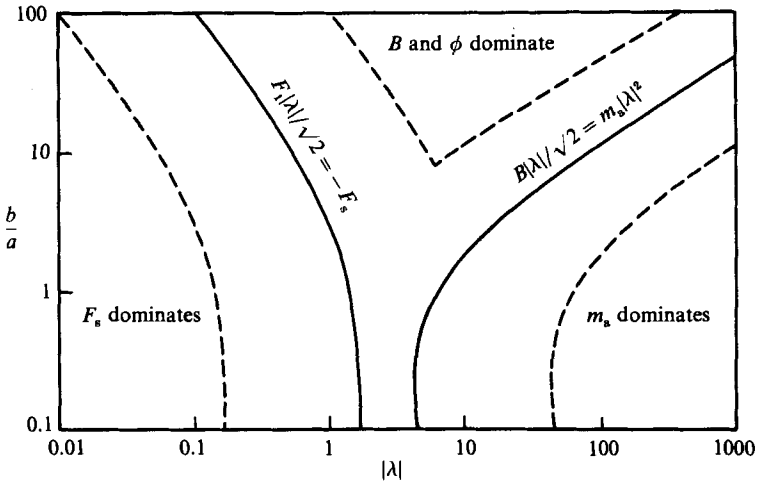

FIGURE 6. The regions of different behaviour in the parameter space of $|\lambda|$ and b/a. The dashed lines are separated from the solid lines by a factor of 10.

the flow is essentially quasi-steady in the neighbourhood of the body and the force is dominated by the steady Stokes drag. At very high frequencies, the potential-flow limit is virtually reached and the force is dominated by the virtual mass term. There is a third region of simple behaviour in which the flow is locally two-dimensional near the body, the ends of the body and the far field being relatively unimportant, and the force is dominated by the generalized Basset and phase-varying forces. The extreme limit of these flows has been discussed by Batchelor (1954) and Hasimoto (1955). These workers considered infinite cylinders where the effect of the external pressure gradient does not contribute to the unsteady viscous layer and the shear stress is simply a modification of (2) to account for an arbitrary uniform cross-sectional geometry. The second and fourth terms in (77) are an extension of this concept to elongated bodies with slowly varying cross-sectional area. The boundaries of these regions of different behaviour are shown in figure 6.

6. Inversion of the Laplace transform

If we consider the force on the spheroid in arbitrary motion with velocity $W(t)$, then the differential equation for $\Psi(\boldsymbol{r}, t)$, is

$$\mathrm{E}^4\Psi - \mathrm{E}^2\Psi_t = 0, \tag{78}$$

We now define a Laplace transform over time

$$\mathscr{L}[f(t)] = \bar{f}(s) = \int_0^\infty \mathrm{e}^{-st} f(t)\,\mathrm{d}t \tag{79}$$

so that $\bar{\Psi}(\boldsymbol{r}, s)$ satisfies the equation

$$\mathrm{E}^4\bar{\Psi} - s\mathrm{E}^2\bar{\Psi} = \Psi(\boldsymbol{r}, 0). \tag{80}$$

If the fluid is initially at rest, $\Psi(\boldsymbol{r}, 0) = 0$, so that (80) becomes the same as (23) with $\bar{\Psi}(\boldsymbol{r}, s)$ replacing $\psi(\boldsymbol{r}, c^2)$. If lengthscale a had been used from the beginning in (23),

c^2 would be replaced by λ^2. The force on the body $\mathscr{F}_{\mathrm{H}}(t)$ transforms in the same way, so the correlation (77) would give

$$-\bar{\mathscr{F}}_{\mathrm{H}} = \left[F_{\mathrm{S}} + Bs^{\frac{1}{2}} + m_{\mathrm{a}}\, s + \frac{F_1 - B}{z_0 + s^{\alpha}} z_0\, s^{\frac{1}{2}}\right] \bar{W}(s), \tag{81}$$

with $z_0 = \lambda_0^{2\alpha}$. The Laplace transform may be inverted to give

$$-\mathscr{F}_{\mathrm{H}}(t) = F_{\mathrm{S}}\, W(t) + \pi^{-\frac{1}{2}} B \int_0^t \frac{\mathrm{d}W}{\mathrm{d}\tau} (t-\tau)^{-\frac{1}{2}}\, \mathrm{d}\tau + m_{\mathrm{a}} \frac{\mathrm{d}W}{\mathrm{d}t} + (F_1 - B) \int_0^t \frac{\mathrm{d}W}{\mathrm{d}\tau} G(t-\tau)\, \mathrm{d}\tau. \tag{82}$$

In (82) and what follows, the time is made dimensionless using the viscous diffusion time a^2/ν. The first three terms of (82) are the analogue of Basset's (1888) result for a sphere, with the Basset force given by the high-frequency correction, viz. B. The fourth term has no analogue for the case of a sphere, since then $F_1 - B = 0$, and this new term will be considered in detail. The memory function $G(t)$ is much more complicated than the $t^{-\frac{1}{2}}$ term in the Basset force; its Laplace transform is

$$\bar{G}(s) = \frac{z_0}{s^{\frac{1}{2}}} \frac{1}{s^{\alpha} + z_0}. \tag{83}$$

At high frequency, $\bar{G}(s) \sim z_0\, s^{-(\frac{1}{2}+\alpha)}$, so the inverse transform for small times will be $G(t) \sim z_0 [\Gamma(\frac{1}{2}+\alpha)]^{-1} t^{\alpha - \frac{1}{2}}$. In table 1, we see that α is positive and typically lies in the range $0.4 < \alpha < 0.7$. Thus $G(t)$ will always have less singular behaviour for small t than does the Basset memory function $t^{-\frac{1}{2}}$, and for $\alpha \geqslant 0.5$, $G(t)$ will not be singular at all. However, at large t (small frequency) $\bar{G}(s) \sim s^{-\frac{1}{2}}$, so $G(t)$ will have the same behaviour as $t^{-\frac{1}{2}}$.

Although (83) is a simple function of s, its inverse transform is difficult to find in the general case. We shall consider first the two special cases $\alpha = \frac{1}{2}, \alpha = 1$, where the transform is tabulated. In these cases, the inverse transforms are (Oberhettinger & Badii 1973)

$$G_{\frac{1}{2}}(t) = z_0\, \mathrm{e}^{z_0^2} \operatorname{erfc}(z_0 t^{\frac{1}{2}}), \quad \alpha = \tfrac{1}{2}, \tag{84}$$

$$G_1(t) = (-z_0)^{\frac{1}{2}} \mathrm{e}^{-z_0 t} \operatorname{erf}(-z_0 t)^{\frac{1}{2}}, \quad \alpha = 1, \tag{85}$$

The first of these is related to the function called $w(z)$ by Abramowitz & Stegun (1965). $w(z)$ is given in terms of a power series in z and asymptotic inverse power series, and we get

$$G_{\frac{1}{2}}(t) = z_0\, w(\mathrm{i} z_0 t^{\frac{1}{2}}) = \sum_{n=0}^{\infty} z_0 \frac{(-z_0 t^{\frac{1}{2}})^n}{\Gamma(\frac{1}{2}n+1)}, \tag{86}$$

and as $t \to \infty$,

$$G_{\frac{1}{2}}(t) \sim \frac{1}{(\pi t)^{\frac{1}{2}}} \left[1 + \sum_{m=1}^{\infty} (-1)^m \frac{1.3 \ldots (2m-1)}{(2z_0^2 t)^m}\right]. \tag{87}$$

The second function (85) is not dignified with a symbol. In this case Abramowitz & Stegun give

$$G_1(t) = \frac{z_0 2t^{\frac{1}{2}}}{\pi^{\frac{1}{2}}} \sum_{n=0}^{\infty} \frac{2n}{1.3 \ldots (2n-1)} (-z_0 t)^n = z_0 t^{\frac{1}{2}} \sum_{n=0}^{\infty} \frac{(-z_0 t)^n}{\Gamma(n+\frac{3}{2})}. \tag{88}$$

The inverse transform of $\bar{G}_{\alpha}(s)$ is not tabulated for arbitrary values of α, but it can be found quite easily by the following (non-rigorous) method. We write $\bar{G}(s)$ from (83) in the form

$$\bar{G}(s) = z_0\, s^{-\frac{1}{2}-\alpha} (1 + z_0\, s^{-\alpha})^{-1}. \tag{89}$$

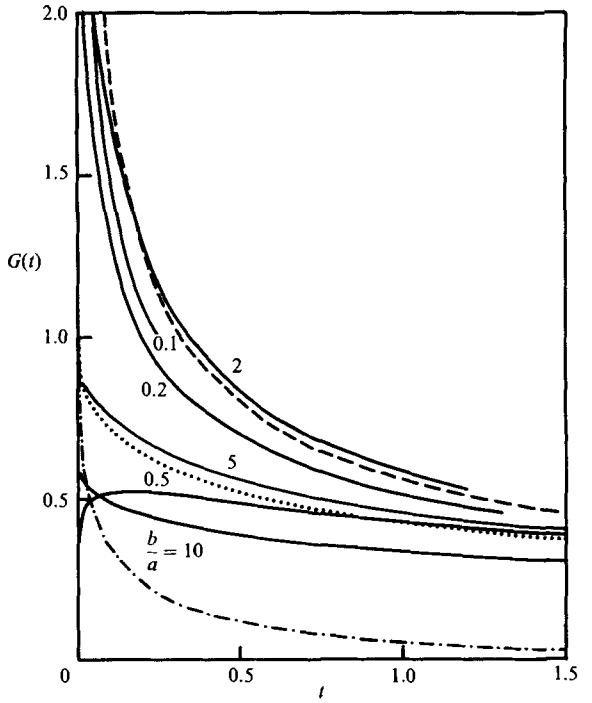

FIGURE 7. The memory function $G(t)$ which appears in the new force term: ——, correlation (92); –·–, asymptotic result for $b/a \approx 1$ (93); – – –, the Basset $1/(\pi t)^{\frac{1}{2}}$ memory function; ·····, crude approximation (94).

Now whenever $|s| > |z_0|^{1/\alpha}$, we can expand the binomial as a convergent power series:

$$\bar{G}(s) = -\sum_{n=0}^{\infty} (-z_0)^{n+1} s^{-[(n+1)\alpha+\frac{1}{2}]}. \tag{90}$$

This form of the Laplace transform $G(s)$ can easily be inverted to give a power series which should be valid at least for small values of t:

$$G_\alpha(t) = z_0 t^{\alpha-\frac{1}{2}} \sum_{n=0}^{\infty} \frac{(-z_0 t^\alpha)^n}{\Gamma[(n+1)\alpha+\frac{1}{2}]}. \tag{91}$$

The power series (91) is uniformly convergent when $\alpha > 0$, which enhances its chances of being reliable. More importantly, it reduces to the forms of (86), (88) when $\alpha = \frac{1}{2}$ or 1, which suggests that it is satisfactory. An additional benefit is that $G(t)$ is real, which is not generally true when $\bar{G}(s)$ is only an approximation, and is a consequence of the form chosen for the correlation (77). If we substitute $z_0 = \lambda_0^{2\alpha}$ in (91), we get the final form:

$$G_\alpha(t) = t^{-\frac{1}{2}} \sum_{n=1}^{\infty} \frac{(-1)^{n+1} (\lambda_0^2 t)^{\alpha n}}{\Gamma[n\alpha+\frac{1}{2}]}. \tag{92}$$

The form of this function is shown in figure 7 for the values of λ_0 and α in table 1. We can obtain a similar form from (7) for the force derived for a nearly spherical body when b/a is close to unity (Lawrence & Weinbaum 1986):

$$G(t) = 2 \sum_{0}^{\infty} \frac{(-3)^n t^{n/2}}{\Gamma(\frac{1}{2}n+1)} \sin[\tfrac{1}{6}(n+1)\pi]. \tag{93}$$

Equation (93) is real since the transform $\bar{G}(s)$ is exact in this case. The function (93) is shown dotted in figure 7.

7. Further discussion

In principle, the method presented herein can be applied to bodies of arbitrary shape. If the solutions for steady Stokes flow and potential flow around a given body are available, the methods used in §3 can be used to generate the $\boldsymbol{F}_1$ and $\boldsymbol{B}$ tensorial coefficients. Furthermore, the behaviour of the correlation approximation (71) is not very sensitive to α and λ_0 except at high frequency where its relative contribution to the force is least, so a reasonable approximation can be obtained for most body shapes by the simpler representation $\alpha = \frac{1}{2}, \lambda_0 = 1$, which allows for a simple inversion for an arbitrary $U(t)$. In this way, we can obtain approximate results for difficult geometries without a full solution of the governing equations. For an arbitrary body, we therefore suggest the approximate form

$$\boldsymbol{F} \approx -\boldsymbol{U}\cdot\left[\boldsymbol{F}_s + \boldsymbol{B}\lambda + \boldsymbol{m}_a\lambda^2 + (\boldsymbol{F}_1 - \boldsymbol{B})\frac{\lambda}{(1+\lambda)}\right] \tag{94}$$

where $\boldsymbol{F}_s$ from (6) is $\boldsymbol{A}$ and $\boldsymbol{F}_1 = \boldsymbol{A}\cdot\boldsymbol{A}$. The approximation given by the last term in (94) is shown in figure 4(*g*). (Note that for oblate spheroids $\boldsymbol{F}$–$\boldsymbol{B}$ is negative.) The accuracy of (94) will be greatest for bodies whose aspect ratio is of order unity and will be least for intermediate values of $|\lambda|$, and for slender bodies. If the approximation shown in figure 4(*g*) is used in place of that in 4(*a*) for a disk-like spheroid of aspect ratio 0.1, the relative error in the total force increases appreciably with a maximum error of about 3% in the range $1 < |\lambda| < 10$. For the needle-like spheroid of aspect ratio 10 considered in figure 4(*f*), the crude approximation is slightly better, leading to a maximum error in the total force of about 2% near $|\lambda| = 1$. We see that the crude approximation (94) works with reasonable accuracy at all frequencies for the spheroids considered with $0.1 < b/a < 10$. We expect that similar accuracy could be obtained for bodies of different shape, provided the aspect ratio remains in the range considered.

We can find the inverse transform of (94) using (84) in which $z_0 = 1$. Thus, the force on a body in arbitrary time-dependent motion with velocity $\boldsymbol{W}(t)$ is

$$-\mathscr{F}(t) \approx \boldsymbol{F}_s\cdot\boldsymbol{W}(t) + \pi^{-\frac{1}{2}}\boldsymbol{B}\cdot\int_0^t \frac{\mathrm{d}\boldsymbol{W}}{\mathrm{d}\tau}(t-\tau)^{-\frac{1}{2}}\,\mathrm{d}\tau + \boldsymbol{m}_a\cdot\frac{\mathrm{d}\boldsymbol{W}}{\mathrm{d}t} + \mathrm{e}(\boldsymbol{F}_1 - \boldsymbol{B})\cdot\int_0^t \frac{\mathrm{d}\boldsymbol{W}}{\mathrm{d}\tau}\,\mathrm{erfc}\,[(t-\tau)^{\frac{1}{2}}]\,\mathrm{d}\tau. \tag{95}$$

Whilst the functional forms of (95) and (7) appear similar, the fourth terms in these two expressions for the force represent different types of corrections. Relation (7) is an exact asymptotic form for near spheres only, while (95) is a more general approximation for a body of arbitrary aspect ratio. For the perturbed sphere, $\boldsymbol{F}_1$ and $\boldsymbol{B}$ are identical up to $O(\epsilon^2)$. Thus, the fourth term in (94) and (95) vanishes to $O(\epsilon^2)$ if one wishes to use these approximate expressions to describe the near sphere. The fourth term in (7) describes very small corrections to the Stokes-drag and virtual-mass forces which combine in different proportions as λ varies when $\epsilon \neq 0$. In contrast, the fourth term in (94) and (95) describes much larger corrections which arise from the fact that the unsteady component of the damping force has a different magnitude at high and low frequency for non-spherical bodies. This basic difference is apparent in figure 7. We see that the memory function in equation (7) for the perturbed sphere decays very rapidly at long times and exhibits a different behaviour to the $t^{-\frac{1}{2}}$ decay for the correlation approximation (77) from which (95) was deduced.

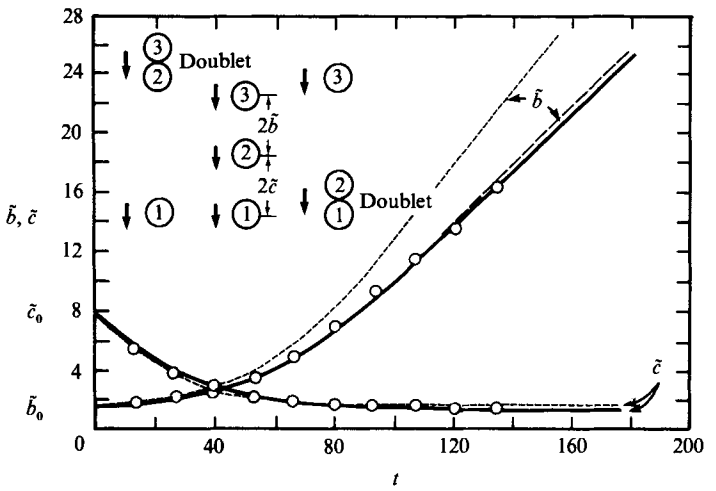

FIGURE 8. The relative motion of three spheres falling under gravity in axisymmetric configuration: $\tilde{b}_0 = 1.63$, $\tilde{c}_0 = 7.38$, $Re = 0.011$: ——, Stokes drag only; – – –, Stokes and Basset terms; ——, all terms. (Reproduced with permission from the Royal Society of London.)

An important result of this work is that for bodies whose aspect ratio is of order unity, the first *three* terms of (94) or (95) provide a very accurate representation for the hydrodynamic force. Thus, the error in the three-term result (8) of Lai & Mockros (1972) is indeed small for nearly spherical bodies. This has far-reaching consequences. In particular, we can infer that a similar functional form would arise for a spherical body in any slightly perturbed non-uniform flow field in which boundaries or other spheres are present. Such a flow field occurs in the case of a group of interacting spheres as discussed by Leichtberg *et al.* (1976). In that work, a chain of three spheres falling along an axis of symmetry was considered. The quasi-steady Stokes resistance tensors were calculated exactly, but the Basset force coefficient for each sphere was assumed to be approximately the same as for an isolated sphere with the same velocity. Figure 8 shows a trailing doublet catching a single leading sphere, then forming a leading doublet which leaves the third sphere behind. Significant deviations from the quasi-steady approximation were obtained, but were unexpectedly accounted for by the isolated-sphere approximation of the Basset force. The resolution of this paradox was one of the motivations for the current work. It is clear from the present theory that the close agreement between the approximate theory and the experimental results of Leichtberg *et al.* may be attributed to the relative insensitivity of the Basset force to geometry when the aspect ratio of the effective combined body is still of order unity. In this case the Basset force for the dipole configuration, see figure 3, is nearly the same for a body of aspect ratio two as it is for a sphere.

For elongated bodies the present results have important implications for the theory of colloidal suspensions. Equation (95) may be used for the hydrodynamic force to find the motion of a sedimenting particle. The equation of motion for the particle is made dimensionless using the terminal settling velocity and the smaller particle dimension. After straightforward simplification one finds that if the coefficient of the steady Stokes-drag term is $\boldsymbol{A}$ the corresponding coefficients of the second and fourth terms in (95) are $\boldsymbol{B}\,Re^{\frac{1}{2}}$ and $(\boldsymbol{A}\cdot\boldsymbol{A}-\boldsymbol{B})\,Re^{\frac{1}{2}}$ respectively. It is clear from the present results that $\boldsymbol{B}$ and $\boldsymbol{A}\cdot\boldsymbol{A}$ are of the same order of magnitude whereas the Stokes-resistance tensor is proportional to $(b/a)\,(1/\log b/a)$. The Basset-force

term in (95) will be $O(\boldsymbol{A}\, Re^{\frac{1}{2}})$ compared to the Stokes-drag term. Typical Reynolds numbers for colloidal suspensions are $O(10^{-4})$. Thus, when $|\boldsymbol{A}| > 100$ the unsteady interactions between the particles are greater than the quasi-steady interaction. This suggests that a major modification to existing theory may be necessary for long slender particulates.

The study of unsteady forces on particles at low Reynolds numbers is emerging as an important extension of the zero-Reynolds-number or quasi-steady problems that have been tremendously popular for the last twenty years. The unsteady forces are important in calculating particle trajectories when streamlines are sharply curved and the flow accelerates strongly, such as in filter membranes (Wang *et al.* 1986). Such situations also arise in turbulent flow where inertial forces prevent particles from following streamlines and contribute to particle dispersion. These areas of application are currently being explored.

This study has been performed in partial fulfilment of the requirements for the Ph.D. degree of C. J. Lawrence from the School of Engineering of the City College of the City University of New York and was supported by the National Science Foundation special 'Creativity' Grant Award ENG 85-00301.

REFERENCES

Abramowitz, M. & Stegun, I. A. 1965 *Handbook of Mathematical Functions*. Dover.

Aoi, T. 1955*a* The steady flow of viscous fluid past a fixed spheroidal obstacle at small Reynolds number. *J. Phys. Soc. Japan* **10**, 119.

Aoi, T. 1955*b* On spheroidal functions. *J. Phys. Soc. Japan* **10**, 130.

Basset, A. B. 1888 *A Treatise on Hydrodynamics*, vol. II. Deighton, Bell & Co.

Batchelor, G. K. 1954 The skin friction on infinite cylinders moving parallel to their length. *Q. J. Mech. Appl. Maths* **7**, 179.

Batchelor, G. K. 1967 *An Introduction to Fluid Dynamics*. Cambridge University Press.

Breach, D. R. 1961 Slow flow past ellipsoids of revolution. *J. Fluid Mech.* **10**, 306.

Chu, L. J. & Stratton, J. A. 1941 Elliptic and spheroidal wave functions. *J. Math. Phys.* **20**, 259.

Clift, R., Grace, J. R. & Weber, M. E. 1978 *Bubbles, Drops and Particles*, p. 293. Academic.

Flammer, C. 1957 *Spheroidal Wave Functions*. Stamford University Press.

Gradshteyn, I. S. & Ryzhik, I. M. 1980 *Table of Integrals, Series and Products*, 4th Edn. Translated from the Russian by Scripta Technica Inc., New York.

Green, G. 1833 Researches on the vibration of pendulums in fluid media. *Trans. R. Soc. Edin.* Reprinted in *Mathematical Papers*. New York: Chelsea Publishing Co. 1970.

Happel, J. & Brenner, H. 1965 *Low Reynolds Number Hydrodynamics*. Prentice-Hall.

Hasimoto, H. 1955 Rayleigh's problem for a cylinder of arbitrary shape. *J. Phys. Soc. Japan* **9**, 611.

Hocquart, R. 1976 Régime instanté d'un liquide dans lequel un ellipsoïde de révolution tourne autour de son axe. *C. R. Acad. Sci. Paris* A **283**, 1119.

Hocquart, R. 1977*a* Régime instanté d'un liquide dans lequel un ellipsoïde de revolution tourne autor d'un axe équatorial. *C. R. Acad. Sci. Paris* A **284**, 913.

Hocquart, R. 1977*b* Movement brownien de rotation d'un ellipsoïde de révolution. Rotation autour de l'axe. *C. R. Acad. Sci. Paris* A **284**, 1421.

Hocquart, R. & Hinch, E. J. 1983 The long-time tail of the angular velocity autocorrelation function for a rigid Brownian particle of arbitrary centrally symmetric shape. *J. Fluid Mech.* **137**, 217.

Kanwal, R. P. 1955 Rotatory and longitudinal oscillations of axisymmetric bodies in a viscous fluid. *Q. J. Mech. Appl. Maths* **8**, 146.

LAI, R. Y. S. 1973 Translatory acceleration of a circular disk in a viscous fluid. *Appl. Sci. Res.* **27**, 441.

LAI, R. Y. S. & MOCKROS, L. F. 1972 The Stokes-flow drag on prolate and oblate spheroids during axial translatory accelerations. *J. Fluid Mech.* **52**, 1.

LAMB, H. 1932 *Hydrodynamics*, 6th Edn, p. 632 *et seq.* Dover.

LAWRENCE, C. J. 1986 Inertial interactions of particles and boundaries in viscous flows. Ph.D. thesis, The City University of New York.

LAWRENCE, C. J. 1988 On the slow transient motion of an arbitrary particle. *J. Fluid Mech.* (Submitted).

LAWRENCE, C. J. & WEINBAUM, S. 1986 The force on an axisymmetric body in linearized, time-dependent motion. *J. Fluid Mech.* **171**, 209.

LEICHTBERG, S., WEINBAUM, S., PFEFFER, R. & GLUCKMAN, M. J. 1976 A study of unsteady forces at low Reynolds number: a strong interaction theory for the coaxial settling of three or more spheres. *Phil. Trans. R. Soc. Lond.* A **282**, 585.

MAGNUS, W., OBERHETTINGER, F. & SONI, R. P. 1966 *Formulas and Theorems for the Special Functions of Mathematical Physics*, vol. 52. Springer.

OBERHETTINGER, F. & BADII, L. 1973 *Tables of Laplace Transforms.* Springer.

SAMPSON, R. A. 1891 On Stoke's current function. *Phil. Trans. R. Soc. Lond.* A **182**, 449.

STOKES, G. G. 1851 On the effect of the internal friction of fluids on the motion of pendulum. *Trans. Camb. Phil. Soc.* **9**, 8.

STRATTON, J. A., MORSE, P. M., CHU, L. J. & HUTNER, R. A. 1941 *Elliptic Cylinder and Spheroidal Wave Functions.* Wiley.

TCHEN, C. M. 1947 Mean value and correlation problems connected with the motion of small particles suspended in a turbulent fluid. Ph.D. thesis, Delft.

WANG, Y., KAO, J., WEINBAUM, S. & PFEFFER, R. 1986 On the inertial impaction of small particles at the entrance of a pore including hydrodynamic and molecular wall interaction effects. *Chem. Engng Sci.* **41**, 2845.